

Correlation between morphology and cathodoluminescence in porous GaP

M. A. Stevens-Kalceff^{a)}

Department of Applied Physics, University of Technology, Sydney. NSW 2007 Sydney, Australia

I. M. Tiginyanu

Laboratory of Low-Dimensional Semiconductor Structures, Institute of Applied Physics, Technical University of Moldova, MD-2004 Chisinau, Moldova

S. Langa and H. Föll

Department of Materials Science, Faculty of Engineering, Christian-Albrechts University, Kaiserstr. 2, 24143 Kiel, Germany

H. L. Hartnagel

Technical University Darmstadt, Merckstr. 25, D-64283 Darmstadt, Germany

(Received 14 August 2000; accepted for publication 9 November 2000)

Porous layers fabricated by anodic etching of *n*-GaP substrates in a sulfuric acid solution were studied by electron microscopy and cathodoluminescence (CL) microanalysis. The morphology of porous layers was found to depend strongly upon the anodization conditions. When the etching process starts at the initial surface, “catacomb-like” pores and current-line oriented pores are introduced at low and high anodic current densities, respectively. After the initial development of either kind of pore, further anodization at the current density of about 1 mA/cm² favors the propagation of pores along $\langle 111 \rangle$ crystallographic directions. The spatial and spectral distribution of CL in bulk and porous samples is presented. A comparative analysis of the secondary electron and panchromatic CL images evidenced a porosity induced increase in the emission efficiency. © 2001 American Institute of Physics. [DOI: 10.1063/1.1337922]

I. INTRODUCTION

Recently, porosity has emerged as an effective tool for controlling the basic properties of semiconductor materials. Bulk Si, for instance, has an indirect band gap and therefore the probability of band-to-band radiative transitions in the material is low. At the same time nanoporous Si obtained by electrochemical dissolution of bulk material in HF-based electrolytes exhibits intense visible luminescence resulting in the development of electroluminescent structures and displays.^{1,2}

Recently, anodic etching techniques have been successfully used for fabricating layers and free-standing membranes of different III–V compounds.^{3–7} Compared with porous Si, III–V materials have a number of important advantages related to the possibility of changing the chemical composition and further extending the fields of applications of porous structures using properties specific to acentricity.⁷ In particular, porous III–V compounds were found to exhibit Fröhlich-type surface-related vibrations with porosity-tuneable frequencies and efficient optical second harmonic generation.^{8–10} The enhanced nonlinear optical response and intense luminescence reported for porous III–V compounds may enable the development of a fully integrated light source and frequency converter subsystem.

So far, most experiments investigating emission characteristics of porous III–V materials have been restricted to photoluminescence (PL). The PL of porous GaP, GaAs, and InP at energies above the band gap of the bulk material has

been attributed to quantum size effects.^{4,9,11–13} Furthermore, a porosity-induced intensification of the near-band-edge emission was observed in gallium phosphide.¹⁴ Nevertheless, no correlation between luminescence properties and morphology features of porous III–V material has been reported yet. In this work, we study the morphology and cathodoluminescence (CL) characteristics of porous layers obtained by electrochemical dissolution of *n*-GaP substrates in an H₂SO₄-based electrolyte. We report drastic modification in both morphology and CL intensity, of porous gallium phosphide layers with changing anodization conditions. The results of the CL microanalysis indicate the possibility of controlling the spatial distribution of emission in porous GaP.

II. EXPERIMENTAL DETAILS

Wafers [(100)-oriented *n*-GaP] cut from Czochralski-grown S-doped ingots were used in this work. The free electron concentration in the as-grown substrates was 5×10^{17} cm⁻³ at 300 K. The anodization was carried out in a double-room electrochemical cell. A four electrode configuration was used: a Pt reference electrode in the electrolyte, a Pt reference electrode on the sample, a Pt counter electrode, and a Pt working electrode. The electrodes were connected to a Keithley 236 Source Measure Unit.

The anodic etching was carried out in 0.5 M H₂SO₄ aqueous electrolyte in both the potentiostatical and galvanostatical regimes. The electrolyte was pumped in a continuous mode through both rooms of the electrochemical cell with the help of a peristaltic pump. The temperature was kept

^{a)}Electronic mail: Marion.Stevens-Kalceff@uts.edu.au

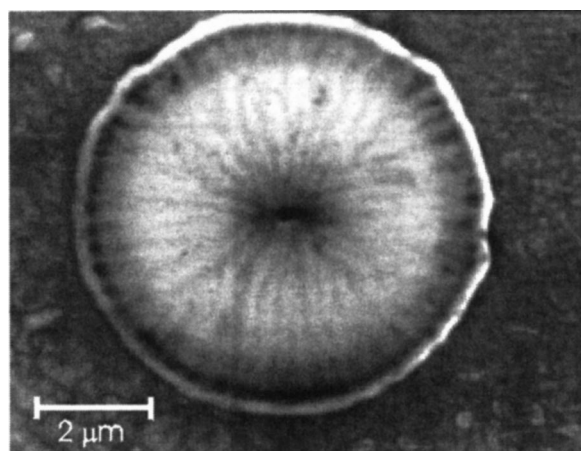


FIG. 1. SEM micrograph of the top surface of a GaP sample anodically etched for 10 min at a constant voltage of +10 V.

constant at $T=23\text{ }^{\circ}\text{C}$ with the help of Julabo F25 thermostat. The area of the sample exposed to the electrolyte was 0.12 cm^2 .

The CL experiments were performed in a scanning electron microscope (SEM) equipped with Oxford Instruments MonoCL2 cathodoluminescence imaging and spectral analysis system, and cryogenic specimen stages. CL and SEM images were taken from the same sample areas for comparison. The CL was excited with a continuous electron beam at normal incidence, and measured using a retractable parabolic mirror collector. CL spectra were collected over the wavelength range 250–900 nm using a Hamamatsu R943-02 high sensitivity photomultiplier with a 1200 line/mm grating, blazed at 550 nm. The CL spectra were collected over a range of beam energies ($E_b=15\text{--}30\text{ keV}$) and beam currents ($I_b=0.25\text{--}100\text{ nA}$) and from $\sim 7000\text{ }\mu\text{m}^2$ regions to reduce electron beam induced effects. The spectra were converted from wavelength to energy space, and corrected for total instrument response.

III. RESULTS AND DISCUSSION

SEM images presented in Figs. 1 and 2(a) show the development of porous regions in *n*-GaP samples subjected to anodic etching under potentiostatic conditions for 10 and 120 min, respectively. In both cases a constant voltage of +10 V was applied to the sample. At the beginning of the process the etching starts at surface imperfections consistent with earlier reports.^{3,6} After initial pitting of the surface, further dissolution proceeds in directions both perpendicular and parallel to the surface. A pore starting at a surface imperfection and growing along a current line or along a definite crystallographic direction is called a primary pore. Pores originating at the surface of a primary pore and propagating away from it are called secondary pores. The development of secondary pores occurs underneath the initial surface. As one can see from Fig. 1, the secondary pores in *n*-GaP propagate radially away from the primary pore, forming a symmetric set of catacombs. Since the etching proceeds at the same rate in all directions, the boundary of the porous region, or, in other words, the porous domain, is circular.

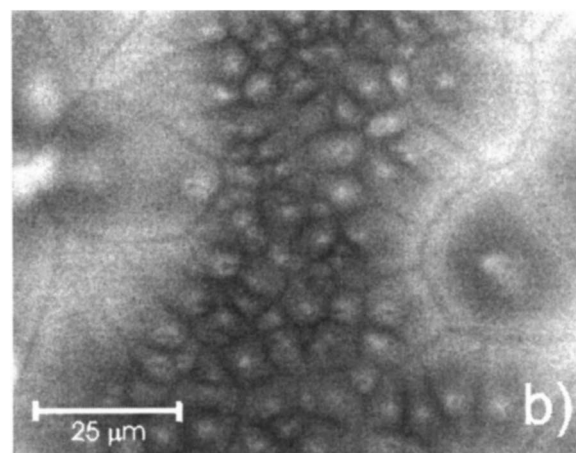
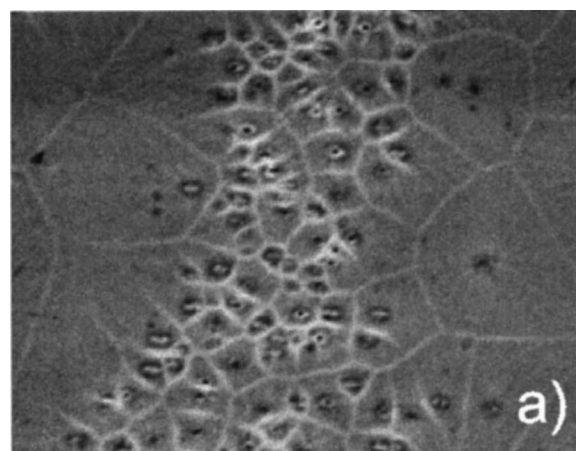


FIG. 2. (a) SEM and (b) panchromatic CL images taken from the top surface of a GaP sample anodically etched for 120 min at a constant voltage of +10 V. Beam energy is 15 keV, beam current is 0.025 nA.

Following etching for an extended period, the secondary pores from different domains eventually meet, leaving nearly straight walls between neighboring porous domains [Fig. 2(a)]. The thickness of these walls is defined by twice the thickness of the surface depletion layer during anodization.³ As can be seen in Fig. 2(a), the lateral dimensions of porous domains depend upon the local density of surface imperfections (e.g., dislocations) initiating the formation of primary pores.

Figure 2(b) is a panchromatic CL image taken from the same region of the as-anodized *n*-GaP sample. It clearly shows a porosity-induced increase of the emission efficiency of gallium phosphide. The light areas in the panchromatic CL image result from enhanced luminescence collected for wavelengths between 250 and 900 nm, with response maximized at $\sim 550\text{ nm}$ (2.25 eV). There is good correlation between enhanced CL emission (lighter areas) in the panchromatic CL image and porous domains in the SEM image. The walls between porous domains are less luminescent and, therefore, are easily distinguished in Fig. 2(b) as dark lines.

To demonstrate the dependence of the emission efficiency upon the degree of porosity, a panchromatic CL image was taken from a sample rendered porous under etching conditions when the applied voltage was temporarily varied between 5 and 15 V. Modulation of the applied voltage is

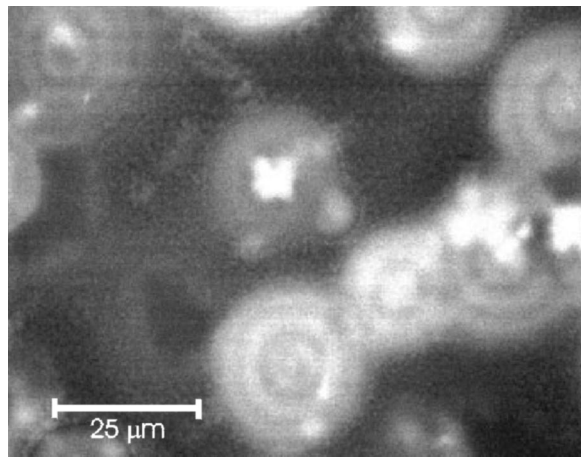


FIG. 3. Panchromatic CL image taken from the top surface of a GaP sample anodized under temporary variations of the applied voltage from +5 to +15 V. Beam energy is 15 keV, beam current is 1 nA.

accompanied by increases and decreases in the anodic current density that cause synchronous modulation of the degree of porosity.⁶ As one can see from Fig. 3, succession of voltage increases and decreases during anodic etching leads to the observation of annular bright and dark tracers around most of the observed etch pits. Note that the dark areas in Fig. 3 correspond to regions unaffected by anodization.

In Fig. 4, CL spectra from bulk and porous GaP fabricated at a constant voltage of +10 V are shown. The spectra are dominated by a broadband at ~ 1.5 eV and a lower intensity band at ~ 2.25 eV. It was found that increasing the beam power (i.e., $E_b I_b$) increased the intensity of the emission at 2.25 eV in absolute terms and relative to the ~ 1.5 eV

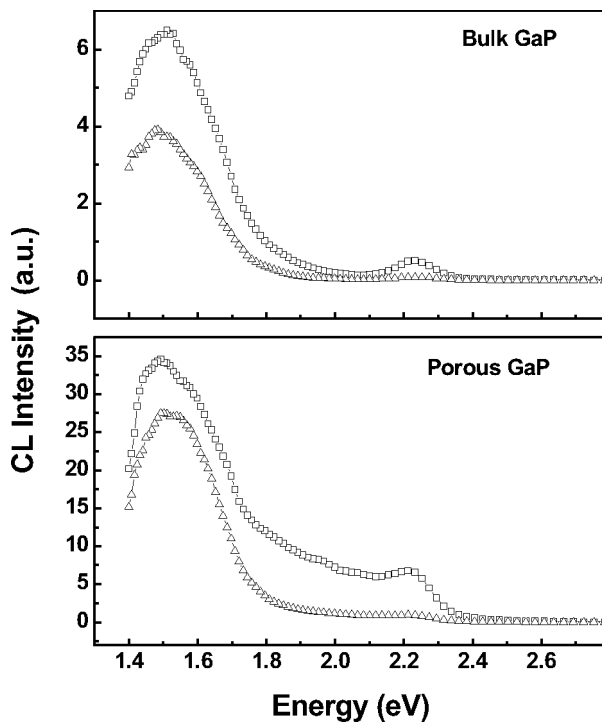


FIG. 4. CL spectra of bulk and porous GaP measured at accelerating voltage of 25 keV and current intensities 10 nA (triangles) and 50 nA (squares).

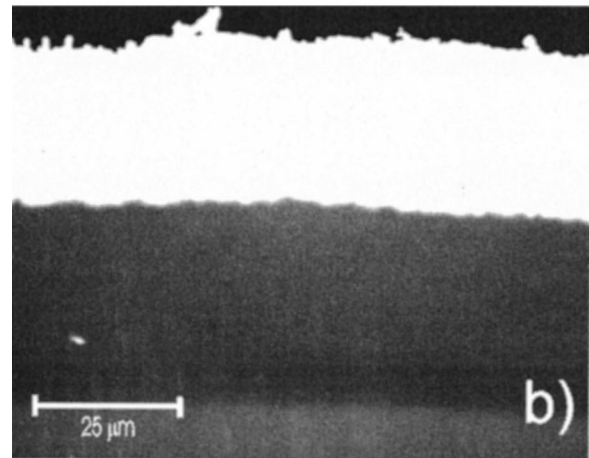
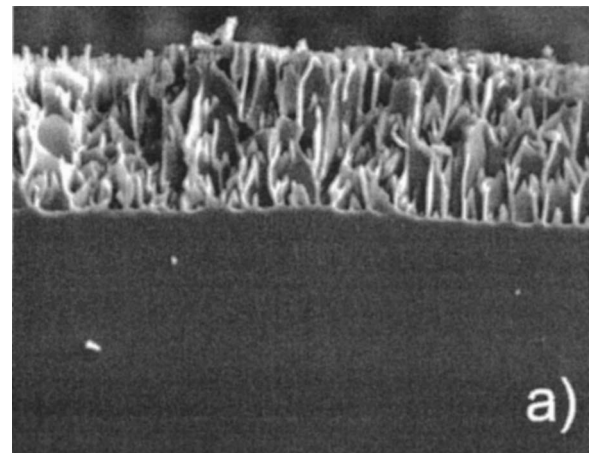


FIG. 5. (a) SEM and (b) panchromatic CL images in cross section taken from a sample anodized galvanostatically at two current densities: $j_1 = 80$ mA/cm² for 60 min and $j_2 = 1$ mA/cm² for 240 min.

emission in both bulk and porous GaP. These two broad emission bands may be attributed to sulfur and some residual impurities including C, O, Zn, and Cd.¹⁵ The emission observed at ~ 2.25 eV has been investigated by a number of groups^{16–18} and associated with radiative recombination at sulfur and carbon atoms on phosphorous sites. Note that, according to the earlier published data on luminescence, deep level transient spectroscopy and optically detected magnetic resonance in *n*-GaP,^{19,20} the 1.5 eV band has been attributed to the radiative recombination of nonequilibrium carriers via donor–acceptor pairs, the donor being a shallow center.

Further evidence of the impact of porosity upon the luminescence efficiency was obtained when studying samples prepared under galvanostatic etching conditions at different anodic current densities. Figure 5 shows SEM and CL images in cross section taken from a sample subjected to successive anodization steps at two current densities: $j_1 = 80$ mA/cm² for 60 min and $j_2 = 1$ mA/cm² for 240 min. Etching at high anodic current density leads to the formation of the so-called current-line oriented pores which are quasi-uniformly distributed and grow inside the sample at nearly the same rate [Fig. 5(a)]. Under these conditions the high density of etching pits at the initial surface excludes the for-

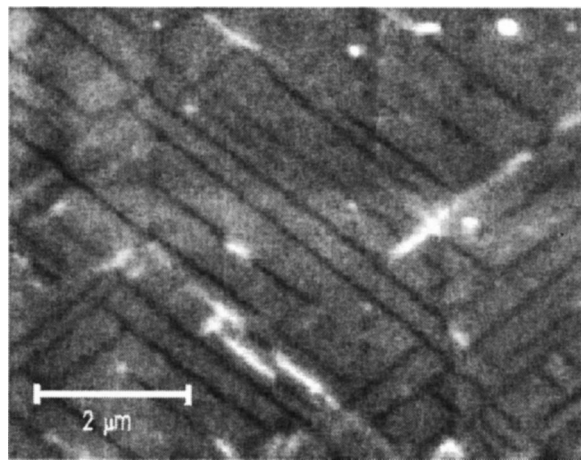


FIG. 6. SEM image in cross section taken from the porous layer produced at current density $j_2 = 1 \text{ mA/cm}^2$ for 240 min (see Fig. 5).

mation of porous domains. When the current density is switched down to 1 mA/cm^2 , the rate of dissolution and the degree of porosity sharply decreased. Somewhat surprisingly, the pores in this case grow along specific crystallographic directions, namely along $\langle 111 \rangle$ directions (Fig. 6).

In full agreement with the data obtained on potentiostatically anodized samples, the higher the degree of porosity, the higher the CL intensity. As one can see from Fig. 5(b), the top layer fabricated at the current density j_1 is more luminescent in comparison with the second layer produced at current density j_2 . Even nonuniformities in the thickness of the top porous layer and small particles related to the cleavage process are clearly distinguished in the CL image. The CL spectra from both layers show luminescence in the near infrared region with the band maximum at about $\sim 1.5 \text{ eV}$ when excited by a low-current electron beam (Fig. 7). The near-band-edge CL at $\sim 2.25 \text{ eV}$ was observed at high beam currents. Under intense excitation, however, the CL from the porous layers was considerably attenuated by the electron beam. The CL attenuation with the time is illustrated in Fig. 8.

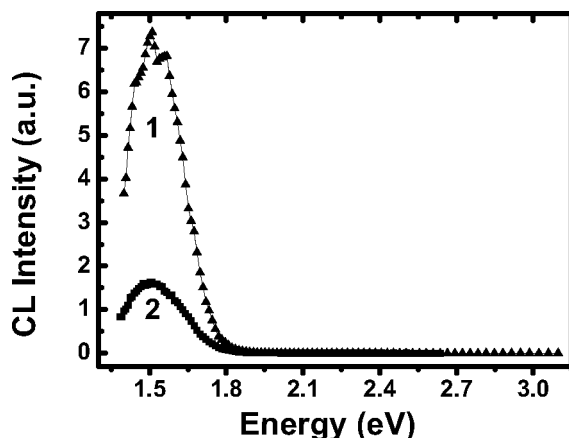


FIG. 7. CL spectra of porous layers produced at current densities $j_1 = 80 \text{ mA/cm}^2$ (curve 1) and $j_2 = 1 \text{ mA/cm}^2$ (curve 2). The beam energy is 15 keV, beam current is 0.025 nA.

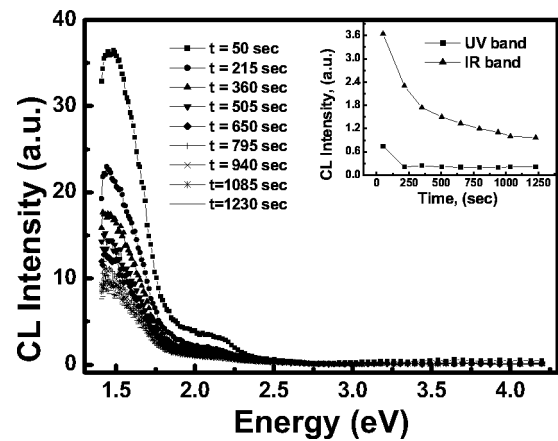


FIG. 8. The time evolution of CL attenuation. The inset shows the time dependence of the intensities of the near infrared (1.5 eV) band and UV emission (integrated from 2.75 to 4.2 eV). The beam energy is 25 keV , beam current is 50 nA .

Degradation of luminescence in bulk GaP and GaP-based light emitting diodes under neutron irradiation, intense laser excitation, etc., has been studied extensively for many years.^{21–23} Particle irradiation usually results in the introduction of nonradiative recombination centers, attenuating the luminescence. However, for beam currents (I_b) greater than 50 nA , the emission in the porous specimens is much more susceptible to beam damage than in as-grown GaP. It is therefore possible that the pronounced CL attenuation in porous GaP is due to irradiation-stimulated out-diffusion of radiative centers. In porous layers possessing a high surface-to-volume ratio stimulated out-diffusion of impurities should obviously be much more significant than in bulk material.

Ultraviolet luminescence from porous GaP has been reported in the literature previously.^{9,11} Broad, very low intensity emission at energies higher than 2.75 eV was occasionally observed in our present porous samples (Fig. 8). This emission is sensitive to irradiation and is very rapidly attenuated by it (see inset in Fig. 8). Currently, there are two possible reasons for the occurrence of UV emission. According to the SEM analysis, the dimensions of the main structural entities of the porous layers are of the order of 100 nm or higher, and therefore they cannot provide conditions for quantum confinement of free carriers. However, it is feasible that the microporous skeleton may be covered by a thin nanoporous film where the occurrence of quantum size effects is possible. For example, in GaAs, electrochemical etching processes have been shown to result in a wide distribution of porosity, varying from micrometer to nanometer range features.²⁴ If this is the case in our present porous GaP samples, then the relatively rapid attenuation of the UV emission under the action of the electron beam (see inset in Fig. 8) can be attributed to local heating due to the reduced thermal conductivity of the film. The second possible reason for the observation of UV luminescence is the formation during anodic etching of a thin oxide film covering the surface of pores.²⁵ Electron beam induced dissociation/damage of the oxide would account for the attenuation of the emission during irradiation. Further studies are necessary to elucidate the origin of UV emission in porous gallium phosphide.

The results obtained demonstrate the possibility of producing porous layers with three different types of morphology. The “catacomb-like” porosity is introduced under “soft” anodic etching of the as-grown samples. In this case the etching starts at surface defects such as emergent dislocation loops and occurs at relatively low current densities not exceeding a few mA/cm² under constant voltage within +5 to +15 V. The symmetric distribution of secondary pores propagating radially away from the primary pore (Fig. 1) seems to reflect the distribution of lattice strain around the dislocations.

The electrochemical dissolution at high current densities is called “shock”-type anodization. A high anodic current is supplied by a high applied voltage which, in its turn, provides conditions for a large band bending. The holes necessary for material dissolution can then be generated by tunneling of electrons at the surface from the valence band to the conduction band.^{3,26} The pores grow along the current lines and the crystallographic orientation of sample proves to have no influence upon the porous layer morphology. The degree of porosity is entirely defined by the anodic current density and the substrate conductivity.

The switch from dissolution at high current density to anodization under soft conditions (e.g., at the current density of about 1 mA/cm²), gives rise to a new type of morphology where the pores are oriented preferentially along crystallographic directions $\langle 111 \rangle$, as can be seen in Fig. 6. This kind of morphology can also be obtained at depth in porous layers under etching conditions which result in formation of catacomb-like porosity in the vicinity of the initial surface. We found that a decrease in anodic current density up to 1 mA/cm² after the porous domains meet favors further growth of pores along $\langle 111 \rangle$ crystallographic directions.

Let us consider the possible origin of the porosity-induced CL intensification in *n*-GaP. The CL emission from the edges of topographical features may be enhanced relative to that observed from a flat bulk specimen, due to geometric effects. Comparison of SEM and CL micrographs from porous regions of GaP show that the enhanced CL emission spatially extends beyond the edges of the pores, and therefore cannot wholly be attributed to geometric effects (for example, see Fig. 2). Observation of intense luminescence, in spite of the high surface-to-volume ratio, implies that the pore surfaces are passivated. Taking into account the composition of the electrolyte, sulfur may be considered as a possible candidate for *in situ* passivation of the porous GaP layers. Sulfur was recently identified as one of the most important surface passivators in III–V compounds.²⁷ Further, electrochemical dissolution of *n*-type semiconductor materials is known to preferentially remove the dislocations and other lattice imperfections^{3,28} which may play the role of nonradiative recombination centers. Reduction in the density of nonradiative recombination centers accompanied by *in situ* surface passivation may explain qualitatively the observed increase in CL intensity induced by porosity.

IV. CONCLUSION

Anodic current density has been found to be the main parameter defining the morphology of porous layers pro-

duced by electrochemical etching of (100)-oriented *n*-GaP substrates in aqueous electrolyte of sulfuric acid. We have established that, depending upon the etching conditions, porous layers with three different types of morphology can be formed including catacomb-like, current-oriented, and crystallographically oriented pores. The growth of pores along the current lines takes place at high anodic current densities. At low anodic current densities, we observed a pronounced anisotropy of anodic etching. When the anodization process is switched on, the dissolution starts at surface imperfections and further proceeds in directions both perpendicular and parallel to the initial surface. The topography of pores propagating in lateral directions seems to reflect the spatial distribution of lattice strain caused by the presence of imperfections. After the development of current-oriented or catacomb-like pores, it is possible to initiate the growth of pores along $\langle 111 \rangle$ crystallographic directions just by decreasing anodic current density. The orientation of pores along the strain lines or along definite crystallographic directions reflects the anisotropy of etching that is manifested at low anodic current densities.

In spite of the huge surface inherent to anodized samples, porosity was found to intensify the CL. Porous domains of GaP were imaged using CL microanalytical techniques. By changing anodic etching conditions, we achieved a synchronous spatial modulation of both degree of porosity and CL intensity. Under electron beam excitation at high current densities, an attenuation of the emission was observed in porous layers and attributed to the irradiation-stimulated out-diffusion of radiative centers.

ACKNOWLEDGMENTS

The authors would like to thank Dr. J. Carstensen and M. Christophersen for fruitful discussion. I. M. T. gratefully acknowledges the support by the Alexander von Humboldt Foundation. M. A. S-K. gratefully acknowledges the support from the Australian Research Council, and technical support from UTS staff.

¹A. G. Cullis, L. T. Canham, and P. D. J. Calcott, *J. Appl. Phys.* **82**, 909 (1997).

²P. M. Fauchet, *IEEE J. Sel. Top. Quantum Electron.* **4**, 1020 (1998).

³B. H. Erne, D. Vanmaekelbergh, and J. J. Kelly, *J. Electrochem. Soc.* **143**, 305 (1996).

⁴T. Takizawa, Sh. Arai, and M. Nakahara, *Jpn. J. Appl. Phys., Part 2* **54**, L643 (1994).

⁵P. Schmuki, J. Fraser, C. M. Vitus, M. J. Graham, and H. S. Isaacs, *J. Electrochem. Soc.* **143**, 3316 (1996).

⁶I. M. Tiginyanu, C. Schwab, J.-J. Grob, B. Prevot, H. L. Hartnagel, A. Vogt, G. Irmer, and J. Monecke, *Appl. Phys. Lett.* **71**, 3829 (1997).

⁷I. M. Tiginyanu and H. L. Hartnagel, in *GAAS'99 Conference Proceedings*, Munich, Germany, Oct. 4–5, 1999 (Miller Freeman, New York, 1999), pp. 194–199.

⁸I. M. Tiginyanu, G. Irmer, J. Monecke, and H. L. Hartnagel, *Phys. Rev. B* **55**, 6739 (1997).

⁹K. Kuriyama, K. Ushiyama, K. Ohbora, Y. Miyamoto, and S. Takeda, *Phys. Rev. B* **58**, 1103 (1998).

¹⁰I. M. Tiginyanu, I. V. Kravetsky, G. Marowsky, J. Monecke, and H. L. Hartnagel, *Phys. Status Solidi B* **221**, 557 (2000).

¹¹A. Anedda, A. Serpi, V. A. Karavanski, I. M. Tiginyanu, and V. M. Ichizli, *Appl. Phys. Lett.* **67**, 3316 (1995).

¹²P. Schmuki, D. C. Lockwood, H. J. Labbe, and J. M. Fraser, *Appl. Phys. Lett.* **69**, 1620 (1996).

- ¹³P. Schmuki, L. E. Erickson, D. J. Lockwood, J. W. Fraser, G. Champion, and H. I. Labbe, *Appl. Phys. Lett.* **72**, 1039 (1998).
- ¹⁴A. I. Belogorokhov, V. A. Karavanskii, A. N. Obraztsov, and V. Yu. Timoshenko, *JETP Lett.* **60**, 274 (1994).
- ¹⁵A. E. Yunovich, *Radiative Recombination in Semiconductors* (Nauka, Moscow, 1972), p. 304.
- ¹⁶P. J. Dean, C. J. Frosch, and C. H. Henry, *J. Appl. Phys.* **39**, 5631 (1968).
- ¹⁷P. J. Dean, J. D. Cuthbert, and R. T. Lynch, *Phys. Rev.* **179**, 754 (1969).
- ¹⁸A. T. Vink, A. J. Bosman, J. A. W. van der Does de Bye, and R. C. Peters, *Solid State Commun.* **7**, 1475 (1969).
- ¹⁹Yu. Ishikawa, Yo. Hayashi, and N. Itoh, *J. Appl. Phys.* **65**, 2035 (1989).
- ²⁰O. O. Awadelkarim, M. Godlewski, and B. Monemar, *Mater. Sci. Forum* **38–41**, 821 (1989).
- ²¹P. Daniel Dapkus and C. H. Henry, *J. Appl. Phys.* **47**, 4061 (1976).
- ²²C. E. Barnes, *J. Appl. Phys.* **48**, 1921 (1977).
- ²³K. Zdansky, J. Zavadil, D. Nohavica, and S. Kugler, *J. Appl. Phys.* **83**, 7678 (1998).
- ²⁴D. J. Lockwood, P. Schmuki, H. J. Labbe, and J. W. Fraser, *Physica E (Amsterdam)* **4**, 102 (1999).
- ²⁵A. Meijerik, A. A. Bol, and J. J. Kelly, *Appl. Phys. Lett.* **69**, 2801 (1996).
- ²⁶F. M. Ross, G. Oskam, P. C. Searson, J. M. Macaulay, and J. A. Little, *Philos. Mag. A* **75**, 525 (1997).
- ²⁷Z. L. Yuan, X. M. Ding, B. Lai, X. Y. Hou, E. D. Lu, P. S. Xu, and X. Y. Zhang, *Appl. Phys. Lett.* **73**, 2977 (1998).
- ²⁸V. Lehmann, *J. Electrochem. Soc.* **140**, 2836 (1993).